ISSN 1392-1207. MECHANIKA. Vol. 31, No. 6, 2025: 554–566

Structural Analysis of Novel Design Compression Feature Intramedullary Nail System Used in Treatment of Femoral Neck Bone Fracture

Hasan Hüseyin GÖKMEN*, Mustafa TINKIR, Ali ÖZTÜRK*****
**Necmettin Erbakan University, Institute of Natural Sciences Dept. of Mechanical Eng., Konya, Turkey,*
E-mail: hhgokmen1@gmail.com
***Necmettin Erbakan University, Department of Mechanical Engineering, Konya, Turkey,*
E-mail: mtinkir@erbakan.edu.tr (Corresponding Author)
****Necmettin Erbakan University, Department of Mechanical Engineering, Konya, Turkey,*
E-mail: aliozturk@erbakan.edu.tr
https://doi.org/10.5755/j02.mech.32947

1. Introduction

Intramedullary nailing systems have become a standard treatment approach for long bone fractures due to their ability to provide internal stabilization and allow early mobilization. Modern proximal femoral nail (PFN) designs have evolved significantly from earlier fixation systems, with improvements in material selection, biomechanical performance, and surgical application. Despite these developments, complications such as loss of reduction, rotational instability, collapse at the fracture site, and insufficient compression across the femoral neck continue to be reported in clinical practice. Femoral neck fractures remain a common orthopedic injury, particularly in elderly patients, and improper stabilization can lead to nonunion or avascular necrosis. Intramedullary PFN systems are generally preferred over dynamic hip screw systems due to their superior mechanical stability and reduced soft-tissue damage. However, the mechanical behavior of screws inserted into the femoral neck region varies among PFN designs, and the interaction between nail geometry, bone structure, and loading conditions plays a key role in postoperative stability. Recent studies have investigated the biomechanical characteristics of PFN systems through experimental testing and finite element analysis, focusing on material behavior, screw configuration, boundary conditions, and fracture patterns.

Bayraktar et al. [1] studied the elastic and yielding properties of trabecular (soft) and cortical (hard) tissues that make up the human femur. In this study, they assumed that the elastic, stretching and yielding properties of trabecular tissue are similar to cortical tissue. They calibrated for cadaveric human femoral neck (femoral head) specimens from 11 donors using a combination of effective tissue modulus and yield strains, apparent mechanical testing, and specimen-specific, high-resolution, non-linear finite element modelling.

Steinberg et al. [2] experimentally investigated the biomechanical properties of the system consisting of nails, screws and neck screws made of stainless steel alloy according to ASTM F384 named "Standard Specifications and Test Methods for Metallic Angle Orthopedic Fracture Fixation Devices". From biomechanical properties; nail bending strength and stiffness, fatigue properties and hip anchor (EP) strength.

Helwig et al. [3] created a geometry model of the proximal femoral nail with CT-database scanning with images of a real femur bone. After modeling, they performed isotropic material behavior and static (linear) structural analysis with finite element software.

Tupis et al. [4] conducted a study called Comparison of two entry points with the same nails using finite element analysis. They performed this study using finite element analysis to compare the magnitude and average stress field distribution originating from each of the two entry points in the proximal femur during antegrade nailing.

Freitas et al. [5] studied the hip screw-plate system experimentally in their study named “Static Load Test of Modified Sliding Hip Screw”. No information is given about how the design of the screw-plate system discussed is made, only the names of the parts that make up the system are mentioned. System; It consists of an angled plate, pipe geometry fitting, slide screw, locking screw and screw pin.

Bayoglu et al. [6] examined how the boundary conditions applied to the proximal or distal femur in finite element modeling affect the mechanics of the bone and the applied nail. As a result of his literature research, in studies examining the proximal part of the femur, he observed that the distal region of the femur, the femoral mid-diaphysis or distal-condyle regions were fixed, and he stated that the boundary conditions were made more carefully and closer to reality in a limited number of studies.

Filardi [7] developed a nail model with a new geometry design, taking into account the disadvantages of locking screws that provide bone nail stability used in today's intramedullary nailing systems. The design consists of a collar, a shaft and a conical pin on the shaft.

Kadir Gok et al. [8] examined which of the different materials showed the best mechanical performance in triangular fixation used in femoral neck fractures. The materials they consider for the system are stainless steel, titanium and cobalt chromium alloys. While creating the CAD model, they created a solid model from the point cloud they obtained by scanning the femur bone. They made the femoral neck fracture through three-dimensional modeling. The finite element method defined the boundary conditions in their study and assigned the mechanical properties of the materials they discussed to the software they used. As a result of their structural analysis, they saw that the most advantageous material was titanium alloy.

Kwak et al. [9] conducted an experimental study on the biomechanical comparison of three different types of intramedullary nails for fixation of intertrochanteric

fractures of the proximal femur, which is one of the unstable types of neck fractures. These three types of intramedullary nails were separated into 12' groups of 36 composite femurs corresponding to osteoporotic human bone. Osteoporotic human bone is the bone structure of a person with osteoporosis.

Putame et al. [10] performed the design of elastic self-locking nails for intramedullary fracture fixation and numerical analysis to determine their mechanical behavior. In this study, they followed a numerical method to compare the mechanical behavior of two new nail types with reference to a clinically used nail.

Herrera et al. [11] performed a biomechanical investigation of the stability of the intramedullary nail, which was adapted for spiral fractures in the femoral shaft. They constructed a three-dimensional finite element model of the femur with different spiral fracture lengths and spaces. They used a femoral nail with two transversal locking screws, both proximal and distal. They considered the situation immediately after surgery, which confirmed the proper stability of Osteosynthesis.

Wang et al [12] investigated the mechanical behavior of 3 types of systems in order to examine the antirotation for subtrochanteric (close to the femoral neck) fracture types in their study. In their review, they discussed the most suitable of these 3 types of systems in terms of biomechanics. They used the finite element method to make comparisons between these systems. The systems they examined consist of two systems implanted into the femoral cortex tissue surface (plaque), and the other two systems. As a result of their study, they saw that PFNA (Proximal Femur Nail Antirotation) implanted into the bone was more positive in terms of stability.

This study presents a comparative issue on the biomechanical behavior of anterograde and retrograde nailing in supracondylar femoral fractures to determine the best choice of nailing and locking configuration. Thanks to the designed compression screw pair, the nail system is given the ability to compress the two broken parts together and in different scenarios (walking, climbing-down stairs, standing on one leg, sitting, kneeling, etc.). Briefly, it is aimed to examine the mechanical behavior of novel design compression feature intramedullary nail system used in treatment of femoral neck bone fracture in this work. Motivated by this fact, in this study, strength analyses of an innovative intramedullary nail system used in femoral neck fractures caused by some accidents in humans are performed according to different motion scenarios and standards, and important technical findings are obtained. In addition, when the literature studies are examined, it has been seen that there is no study similar to the same design and compression application with the intramedullary nail system discussed in this research. Within the scope of this work; the design of the intramedullary nail system with compression feature, which is used in the treatment of femoral neck fractures and to prevent the rotation of the fractured parts, the numerical modeling of the parts that make up the system and static analysis are carried out. In addition, three-dimensional design models are obtained according to the mechanical properties of the hard (cortex) tissue and soft-spongeous (spongious) tissues forming the femoral bone. Moreover, a fracture profile is designed in the femoral head and the implanted model of the nail system consisting of Ti6Al4V Grade 23 material into the femur bone in order to stabilize the fracture is created. After this stage; structural structure of both the intramedullary nail system and the femur bone using the finite element method according to the resultant forces obtained from the experimental data in the literature and coming to the bone implant system in different movement scenarios (walking, stair climbing-down, standing on one leg, sitting, kneeling and standing up) are carried out, deformation and stress conditions are examined. Two different material models, isotropic and orthotropic, are used in the modeling of the femur bone, and it is concluded that the orthotropic bone model is closer to the results in the literature Additionally, in order to examine the rigidity of the intramedullary nail, three-point bending tests are performed and interpreted according to ASTM F1264 standards.

As a result, the objective of this study, very important technical findings are obtained for the advantageous design of the proximal femoral nail and screws used in the treatment of femoral neck fractures and the biomechanical compatibility of the structure formed by the PFN system with the bone. In this sense, it is expected that the material modeling methods and design techniques used in the study will contribute to the literature for similar implant and hip prosthesis designs.

2. Modelling and Structural Analysis of Proximal Femur Nail System

There are many types of nail systems used in the treatment of femoral neck fractures. These nail systems vary according to the method and number of screws placed in the femoral neck. There are also open surgically implanted plate systems used in femoral neck fractures. Today, mostly nail systems are preferred provided by shake table are towards the right as shown in Fig. 1.

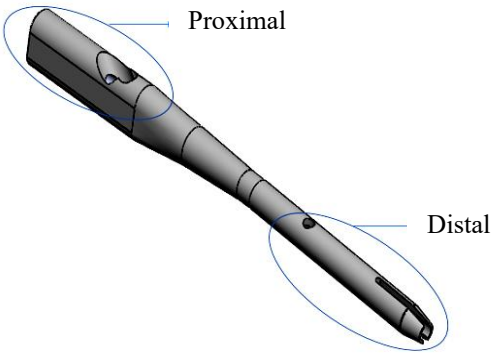

Fig. 1 The proposed proximal femur nail

While creating the proximal femur nail (PFN) system model, the literature is searched, the implant manufacturers are interviewed and the opinions of the doctors are reached. As a result of all these, while designing the system, a design suitable for the anatomical structure of the general femur bone is realized. The nail design starts with an equilateral trapezoidal section proximally and becomes a circular structure distally. The nail length is 200 mm, which provides the advantage of design development for both neck and proximal multiple shaft fractures. The reason for its circular structure is that the medullary canal is a nearly circular cross-section. The outer diameter of the distally circularized section is designed to be 10 mm on average, and diameter configuration can be made according to the cortex tissue thickness in the diaphysis region of the case to be applied.

After the nail has a fixed diameter, it is shaped with a 4° twist in order to be suitable for the general femur bone structure, to facilitate the implantation and to be suitable for the curved geometric in the canal due to the nature of the femur bone. A 5.25 mm diameter deep hole design is made in the nail for the cannulated spindle used in surgical operations. There is a 4.5 mm diameter locking screw hole near the distal part of the nail. In the distal part of the nail, slits are modeled for ease of implantation. In the proximal part of the nail, there is a compression screw slot that will prevent the compression screw pair from slipping, as well as a top screw slot to facilitate the removal of the implant. In addition, there is a pair of holes through which the compression screw pair passes. The proposed PFN is given in Fig. 1. The general assembly of the PFN system consisting nail, compression screw pair, compression screw, crown screw and locking screw are given in Fig. 2.

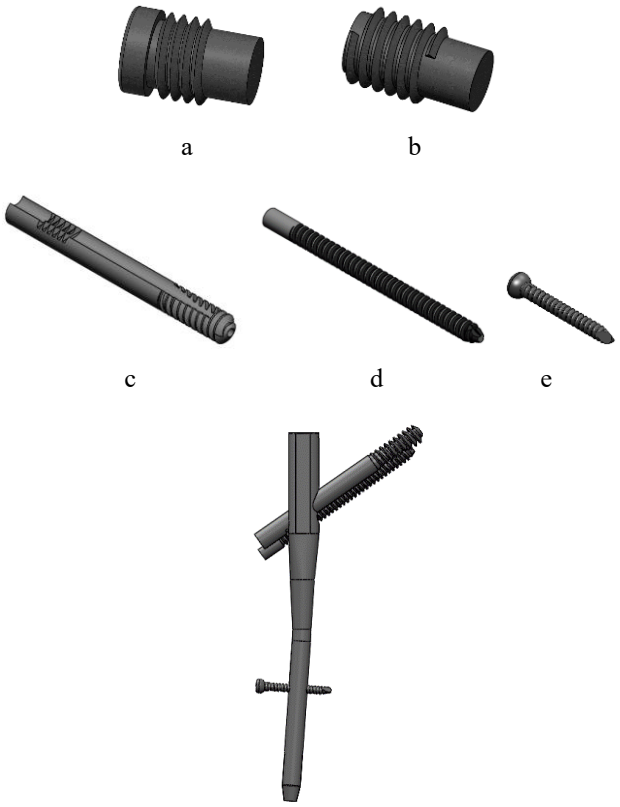

Fig. 2 PFN system components: a – the end screw, b – the compression screw, c – the lag screw, d – the locking screw, e – the compression screw, f – PFN system assembly

The end screw is given in Fig. 2, a, has no mechanical function and is to prevent the cancellous (soft) tissue from advancing into the nail from the proximal part of the nail. This facilitates the removal of the nail. The compression screw is a screw that aims to prevent the mechanical movement and slippage of the compression screw pair, shown in Fig. 2, b. Its design is made to press the lag screw. The diameter of the lag screw, which is one of the screws that make up the compression screw pair, is 11 mm, its length is designed according to the length of the average femoral neck bone, and its length is 105 mm. For adhesion to the cancellous tissue, a design has been made with the surface areas of the grooves increasing towards the tip, it is given in Fig. 2, c. The bottom of the thread, the diameter of the top of the thread, and the radii of the bottom of the thread of the locking screw are standard (ASTM F543) and the length is designed as 41 mm according to the bone model to be used in this study. According to design standards, this screw has a self-tapping feature shown in Fig. 2, d. In addition, a channel in which the other screw pair works is modeled. The length of the compression screw given in Fig. 2, e, which is another screw of the screw pair, is 100 mm and it is intended to work in harmony with the lag screw. The compression screw works on the lag screw and aims to provide compression and fixation of two broken bone fragments. Moreover, PFN system assembly model is seen in Fig. 2, f.

2.1. Modeling of femur bone and implanted

There are different approaches available for generating solid models of the human femur bone. Based on the literature survey, computed tomography (CT) scanning is widely used for constructing anatomically accurate femoral geometries. In the present study, the femur CAD model was generated by optically scanning a 50 cm long left femur specimen, representative of average adult femoral dimensions, using a high-resolution three-dimensional scanning system with a maximum measurement sensitivity of 0.05 mm. The acquired raw scan data were processed and refined to obtain a high-density point cloud representation of the femoral surface, as illustrated in Fig. 3, a-b, respectively. Subsequently, the point cloud data were converted into a watertight surface model and further reconstructed into a solid CAD geometry suitable for finite element discretization. This procedure ensured accurate preservation of anatomical features and geometric continuity required for reliable biomechanical simulations.

A solid model of the femoral bone is created from the point cloud. When it is examined the femur bone, it generally consists of two main tissues as cortex and spangle. From the solid model obtained from the point cloud, these two textures are designed as solid models given in Fig. 4, a-b, respectively.

Fig. 3 Femur bone structure: a – femur bone scan data, b – femur bone point cloud

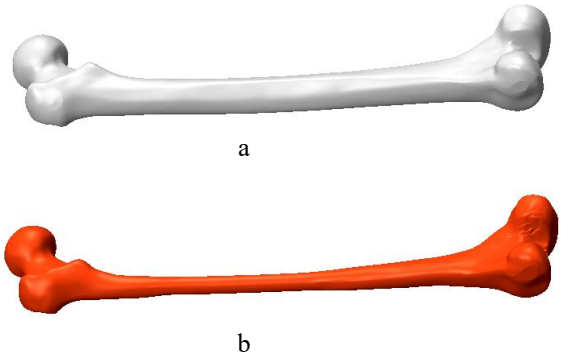

Fig. 4 Bone tissue: a – cortex, b – spangle

Fig. 5 Femoral neck fracture solid model

For the basis of the study, a fracture design is made in the femoral neck in the solid models obtained above is given in Fig. 5.

After the entire solid model design, the nail system is implanted into the femur bone. While this implant is performed, it is done according to the order of the operations performed in the surgeries. According to the actual implanted femur-PFN, the obtained cancellous tissue solid model is remodeled according to the nail system. The cortex tissue is reconstructed according to the actual implanted screws. Femur-PFN system implantation solid models are shown in Fig. 6.

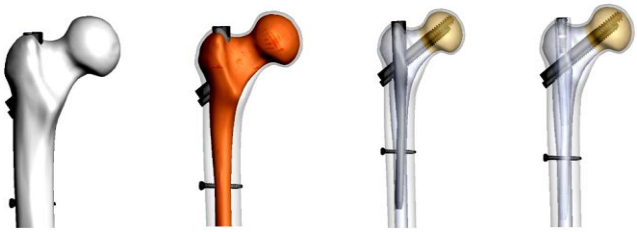

a b c d

Fig. 6 Femur-PFN system implantation solid models: a – native femur anatomy, b – femoral canal preparation prior to nail insertion, c – insertion of the proximal femoral nail, d – final configuration after complete PFN fixation

The mechanical tests required for intramedullary nail systems have been investigated. As a result of this research, the ASTM-F1264 biomechanical test standard has been reached. In the detailed research, in order to obtain CE and ISO 13485 certificates, which is the manufacturer's warranty statement and which is also expressed as the passport of the product, for companies that want to manufacture nails or continue to produce nails in the USA and Europe, or from companies that continue to produce, in certain periods. The requested ASTM-F1264 is the biomechanical test named "Standard Specification and Test Methods for Intramedullary Fixation Devices". When the test standard is examined in detail, it is possible to analyze the test scenario or structurally critical areas in the system, hand calculations, finite element analysis, etc. In the present investigation, both linear elastic and nonlinear elastoplastic material models were employed to accurately capture the mechanical behavior of the nail under the boundary conditions of the standardized nail testing procedure as well as under physiological loading scenarios encountered in clinical applications. The inclusion of nonlinear material behavior is particularly essential due to the presence of localized plastic deformation observed during experimental nail testing and potential in-service loading conditions in the human femur. Therefore, the combined use of linear and nonlinear constitutive models enables a comprehensive evaluation of the structural response of the implant across the full operational loading range. As a biomedical material, the nonlinear material model of Ti6Al4V Grade 23 could not be found as a result of the literature review. Tensile test experimental data for Ti6Al4V Grade23 are obtained by interviewing a representative of a Titanium producer company in Europe.

In the present study, the constitutive behavior of the Ti-6Al-4V ELI material was numerically modeled using the Multilinear Isotropic Hardening approach implemented in the finite element analysis framework. This method enables accurate representation of elastic–plastic material response by approximating the true stress–strain curve with a series of linear segments. To construct the numerical material model, experimental uniaxial tensile test data were employed as the primary input. From these experimental measurements, the true stress, true strain, elastic modulus, elastic strain, and plastic strain values required for the hardening law were obtained. These parameters were calculated by means of the formulations provided in Eqs. (1-5). The resulting piecewise-defined constitutive relationship was subsequently incorporated into the numerical model to simulate the nonlinear deformation behavior of the material under physiological loading conditions.

$$\varepsilon_{true} = ln(1+\varepsilon_{eng}), \tag{1}$$

$$\sigma_{true} = \sigma_{eng}(1+\varepsilon_{eng}), \tag{2}$$

$$E = \sigma/\varepsilon, \tag{3}$$

$$\varepsilon_{elastic} = \sigma_{stress}/E, \tag{4}$$

$$\varepsilon_{plastic} = \varepsilon_{total} - \varepsilon_{elastic}. \tag{5}$$

The modulus of elasticity of Ti6Al4V ELI is calculated by Eq. (3). From the experimental data, the elastic modulus was taken as $E = 104.2$ GPa. Ti6Al4V ELI real-eng. stress-strain graphic is given in Fig. 7.

Ti6Al4V ELI elastic and plastic material models are defined using ANSYS/Workbench program and they are given in Table 1-2, respectively.

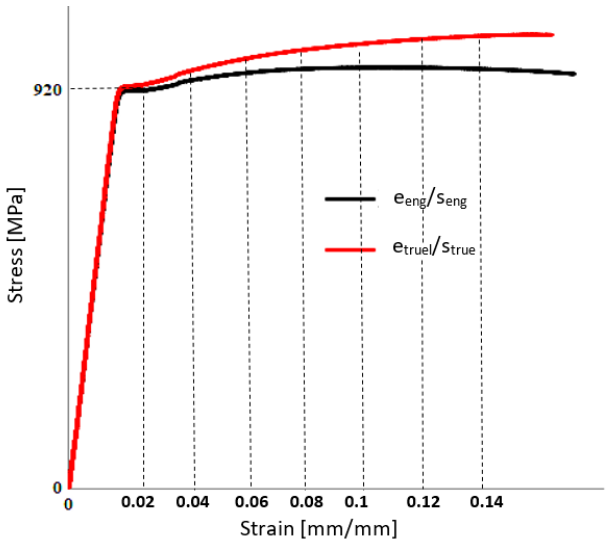

Fig. 7 Stress-strain response of Ti6Al4V ELI

Table 1

Ti6Al4V ELI Elastic Material Model Data

The modulus of elasticity, GPa	Poisson's ratio	Yield stress, MPa
104.2	0.342	920.626

Table 2

Ti6Al4V ELI Plastic Material Model Data

Plastic strain, mm/mm	True stress, MPa
0.00	920
0.01	960
0.02	995
0.05	1070
0.10	1130

If a material has three mutually perpendicular material planes of symmetry, the stiffness matrix is written as follows:

$$\begin{matrix} \frac{1}{E_1} & -\frac{\nu_{21}}{E_2} & -\frac{\nu_{31}}{E_3} & 0 & 0 & 0 \\ -\frac{\nu_{12}}{E_1} & \frac{1}{E_2} & -\frac{\nu_{32}}{E_3} & 0 & 0 & 0 \\ -\frac{\nu_{13}}{E_1} & -\frac{\nu_{23}}{E_2} & \frac{1}{E_3} & 0 & 0 & 0 \\ 0 & 0 & 0 & \frac{1}{G_{23}} & 0 & 0 \\ 0 & 0 & 0 & 0 & \frac{1}{G_{13}} & 0 \\ 0 & 0 & 0 & 0 & 0 & \frac{1}{G_{12}}. \end{matrix}$$

In this study, the numerical model of the cortex and spongios tissue material of the femur bone are defined as orthotropic mechanical constants according to Solorzano et al. [13]. The definition is three modules of elasticity E, three modules of shear G, and three Poisson's ratios ν depending on the radial, circumferential and longitudinal axes. Bergman et al. [14] in their study, realistic loads for testing hip implants, aimed to define realistic load conditions for hip implants based on contact force measurements in vivo and whether current ISO standards actually simulate real loads. In their study, they measured hip contact forces with range-finder hip endoprostheses implanted in 4 subjects with hip calcification during "walking (4 km/h), climbing stairs, descending stairs, standing up, sitting, standing on one leg, kneeling" activities. It has been investigated how the contact forces are measured. It has been observed that the tip of the prosthesis is formed by applying three semiconductor strain gauges to the lower end of the inner wall and connecting it to the 4-channel transmitter, receiving data from the transmitting antenna inside the ceramic ball. Data of subjects using hip contact force in different scenarios are given in Table 3.

Table 3

Data of subjects using hip contact force in different scenarios (Bergman et al. [14])

	Patient 1	Patient 2	Patient 3	Patient 4	Average
Gender	Male	Male	Male	Female	-
Age	55	51	61	76	60
Mass index, kg	87.7	99.9	71.6	81.5	85.1
Activity level	Very High	High	Normal	Low	-

As a result of the experimental measurement, the femoral contact forces taken in "walking (4 km/h), climbing stairs, descending stairs, standing up, sitting, standing on one leg, kneeling" activities are shown in Table 4. Boundary conditions; as a force, the hip contact forces formed in the activities of "walking (4 km/h), climbing stairs, descending stairs, standing up, sitting, standing on one leg, kneeling" in Table 4, three resultant forces for each activity, parameter (7 activities) according to the axes shown in Fig. 8 and the distal end is defined as the fixed support. Material properties of femur bone is given in Table 5.

Femur-PFN implanted system boundary conditions and cortex-spongios inter-tissue connection model are given in Fig. 9, a-b, respectively.

In the study, the fracture line is modeled as a "frictional" connection with a friction coefficient of 0.46. Fig.10, a shows the connection model between two broken parts. Additionally, the friction coefficient of 0.42 is modeled as "Frictional" between nail-spongios tissue, lag screw-spongios tissue, lag screw-cortex tissue, compression screw-spongios tissue and compression screw-cortex tissue. The connection model between the bone tissues and the implant is given in Fig. 10, b.

Table 4

Mean peak hip contact force data measured from 4 subjects in different activities (Bergman et al. [14])

Average Peak Forces							
Activity performed	Maximum contact forces, N				Angles, degrees		
	F	*-Fx*	*-Fy*	*-Fz*	*Ax*	*Ay*	*Az*
Walking (4 km/h)	1800	403	249	1736	81.8	13.1	31.8
Climbing the stairs	1900	446	464	1787	75.5	14	46.1
Descending the stairs	2000	370	292	1944	81.5	10.8	38.3
Stand up	1500	420	105	1436	85.8	16.3	14
Sitting	1200	323	-5	1155	90.2	15.6	-0.8
Standing on one leg	1800	203	108	1785	86.5	6.5	28.1
Kneeling	1100	290	39	1060	87.9	15.3	7.7

Table 5

Material Properties of Femoral Bone Tissues (Solórzano et al. [13])

Property	Cortex, MPa	Spongious, MPa
E_x	17000	450
E_y	11000	340
E_z	13000	560
G_{xy}	3800	100
G_{yz}	3500	90
G_{zx}	4000	120
ν_{xy}	0.38	0.25

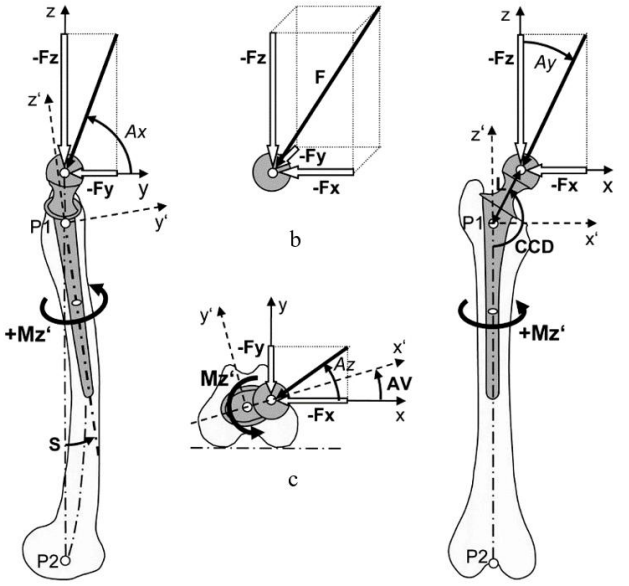

Fig. 8 Femur hip replacement force axis definitions: a – the local force components (*Fx*, *Fy*, *Fz*) and bending moment (*Mz*), b – the resultant load vector *F* into Cartesian components, c – transverse plane representation of force and moment, d – the force axes within the anatomical femoral reference frame including the CCD angle

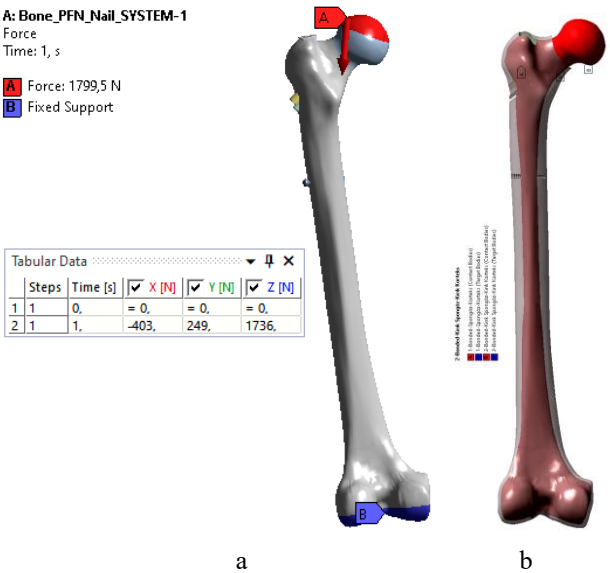

Fig. 9 Femur-PFN implanted system: a – boundary conditions, b – cortex-spongios inter-tissue connection model

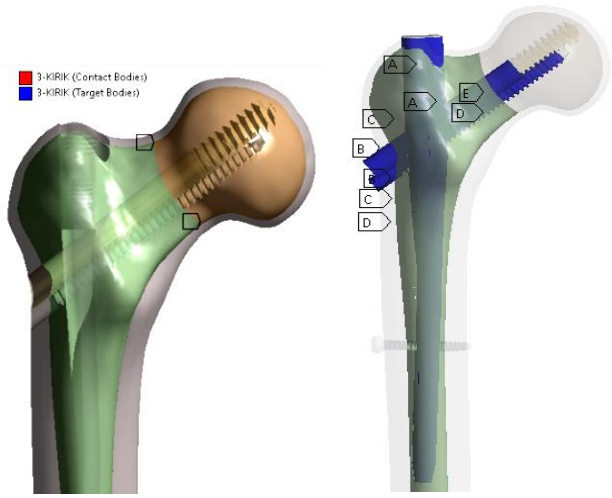

Fig. 10 The connection model bone and implant: a – model between two broken parts, b – the connection model between the bone tissues and the implant

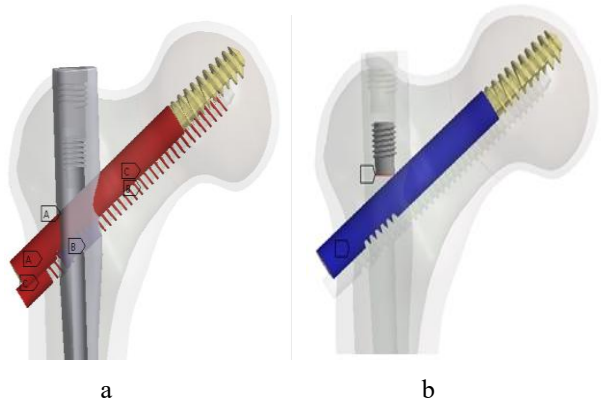

Fig. 11 The connection model implants: a – the connection model between implant and implant, b – the connection model between two screws

Frictional contact is defined between lag screw-nail, compression screw-nail and compression screw-lag screw and the friction coefficient is modeled as 0.23. Frictional contact modeling on screws does not include the thread parts of the screws. Fig. 11, a shows the connection model between implant and implant. It is assumed that there is a very serious friction between the compression screw and the lag screw, which aims to prevent the compression screw pair from slipping, and the distance between these two screws is modeled as "Bonded". Fig. 11, b shows the connection model between these two screws.

All contacts of the spongios tissue–lag screw in the fractured fragment, the spongios tissue–compression screw in the fractured fragment, and the locking screw were modeled as “Bonded”. These contact patterns are shown in Fig. 12. According to the literature research, the boundary conditions and the connection definitions between the elements in this study were modeled realistically. The connections were mainly established between cortical tissues, spongious tissues, fracture lines, and implant–bone interfaces, and a total of 19 distinct contact models were implemented. The bonded contact formulation was selected to represent the fully constrained conditions established after surgical fixation, preventing relative sliding or separation

between contacting surfaces. This approach ensured numerical stability of the finite element solution and allowed accurate transfer of stresses across the bone–implant interfaces. Consequently, the developed contact framework provided a reliable representation of load transmission mechanisms under physiological loading conditions.

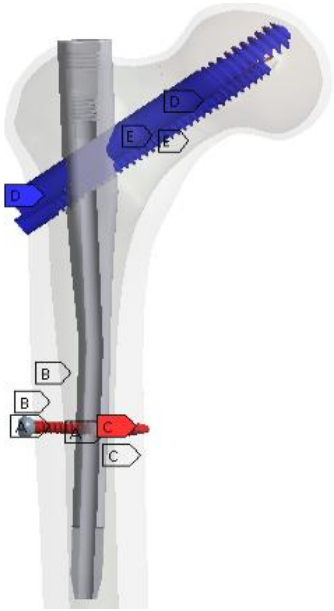

Fig. 12 Screws contact modeling

2.2. Finite element model of the implanted system

In order to statically examine the implanted system, the CAD model of which is created in the SOLIDWORKS program, the parts are converted into a mathematical model (mesh model). In the static analysis study, "body sizing" is used as the mesh method, "face sizing" is used in the detail areas and a regular tetrahedron element mesh geometry is chosen. Element sizes according to the elements that make up the system-mesh method are given in Table 6.

Finite element model of the femur-PFN implanted system is given in Fig. 13.

3. Results and Discussion

Actions such as walking, going down stairs, climbing stairs, standing on one leg, sitting, kneeling are the basic activity movements of people of all ages. When multi-parameter cases such as age, race, gender, height, physical activity, sports history, nutritional habits and most importantly weight are considered, medical implant design can be quite difficult depending on these parameters. In this study, according to the subjects mentioned in Table 3-4, the average body mass is 85.1 kg, the average age is 60, the activity level is normal, the femoral head has a femur bone with a tip of 50 cm from the apex to the distal; walking, climbing the stairs, descending the stairs, stand up, sitting, standing on one leg and kneeling during the activities, the maximum contact force on the femoral head is applied. The forces acting on the femoral head are in three axes, in the range of 0-1 seconds, and are defined to increase linearly. The image of the definitions of the different forces in each activity is not given, but only the definition of the force that comes during walking (4 km/h) is given in Fig. 8. As can be seen in Table 4, the highest load on the vertical axis of the femur is stair climbing, stair climbing, standing on one leg and walking partially.

a b c

Fig. 13 Screws contact modelling: a – surface-meshed femur geometry, b – assembled femur-PFN model including all implant components, c – cross-sectional view of the implanted femur

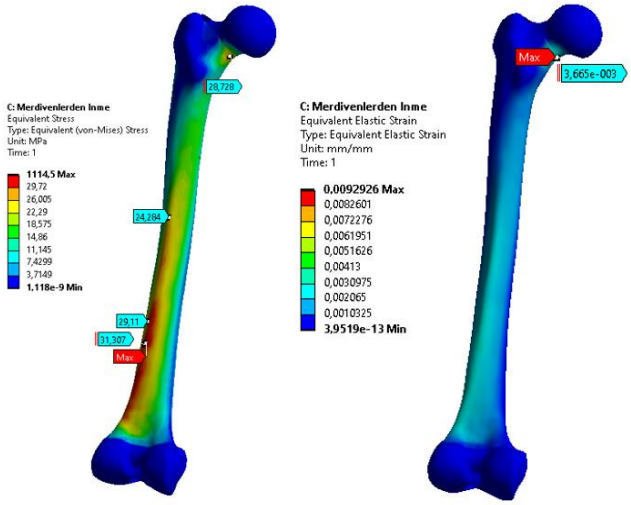

a b

Fig. 14 Femur cortex tissue stress-elastic strain distributions: a – von Mises stress distribution, b – equivalent elastic strain distribution

Table 6
Element dimensions of the elements constituting the implanted system

Mesh method	Cortex tissue	Spongios tissue	Nail	Screws (All)
Body sizing	4 mm	2 mm	2 mm	1 mm
Face sizing	--	1 mm	--	--

Model evaluation was primarily based on von Mises stress results, which provide stable criteria for identifying critical load-bearing regions within the femur–PFN system. These stress distributions enabled the assessment of structural safety and facilitated the determination of potential design improvements for the implant screws as well as the computation of the factor of safety. The equivalent Von Misses stress output in the cortex tissue as a result of the maximum resultant force loading of 2000 N on the femoral head at the time of going down the stairs is as in Fig.14.

Displacement results were examined to verify the consistency of the numerical response with the prescribed boundary conditions and to confirm the overall accuracy of the finite element model. The results of the analysis are evaluated as cortex tissue, spongios tissue and parts of the PFN system, respectively. Considering the loads in each activity, the highest load on the femoral head is the situation of going down the stairs. Moreover, strain distributions were analyzed to support mechanical strength evaluation, following the construction of the femur–PFN CAD model, material assignment, application of load cases representing seven daily activities, definition of bone–implant contact interactions, and mesh discretization prior to solving the numerical model.

The highest stress that occurs in the cortex tissue as a result of a resultant force of 2000 N per femur at the time of stair descent is 31.3 MPa, and it is located in the posterior part of the region in the distal slice of 1/3 of the diaphysis. The maximum stress on the system element is 1114.5 MPa, and the color scale is adjusted to show the tension in the cortex region according to the color scale distribution. When we interpret it according to ultimate tensile strength of bone, 135 MPa (Gök et al. 2017), the resulting stress value of 31.3 MPa is quite low. The elastic strain for cortex tissue is the highest at 0.0036 mm/mm and is in the region below the fracture line in the femoral neck. According to these examinations, the bone shows an elastic behavior in the elastic deformation zone and according to the obtained stress results, the material does not pass into the plastic deformation zone. Again, the stress distributions and strain results in the spongios tissue are investigated according to the same (descend from the ladder) loading conditions. Spongios tissue equivalent stress distribution is given in Fig. 15. Spongios tissue strain distribution is given in Fig. 16.

Examination of the spongios tissue stress distributions indicates that the maximum stress reaches 38.3 MPa and occurs in the regions corresponding to the tooth base of the compression screw. Screw threads are not neglected while CAD modeling is carried out, taking into account the ability of the spongios tissue to regenerate and reproduce over time. Accordingly, the equivalent stress distributions obtained are 0-38.3 MPa; the compact structure of the bone and ultimate tensile strength mentioned in the literature are evaluated as suitable. The maximum elastic strain in spongios tissue is 0.0052 mm/mm.

The stress and strain conditions in the spongios tissue and cortex tissue as a result of loads in other activities were investigated. The results of the stretching occurring in the cortex tissue are given in Table 7. Elastic strain results in cortex tissue are presented in Table 8. The results of the stretching occurring in the spongios tissue are shown in Table 9. Elastic strain results in spongios tissue are given in Table 10. When we look at the forces on the femoral head

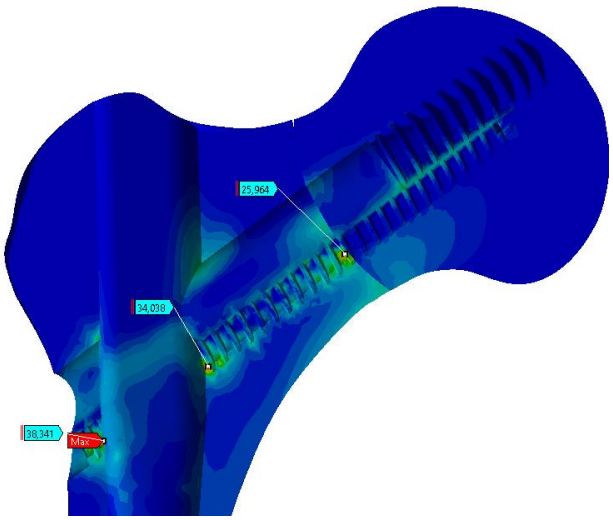

Fig. 15 Femur spongios tissue stress distributions

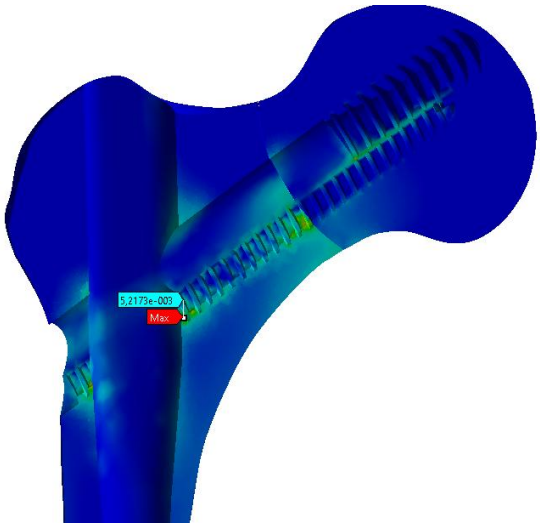

Fig. 16 Femur spongios tissue strain distributions

Table 7
Femur Cortex Tissue Stress Caused by Activities

Cortex tissue			
Activity	**Max. stress zone**	**Max. stress**	**Stress distribution**
Walking (4 km/h)	Diaphysis, 1/3, distal	30.40	0-30.4
Climbing the stairs	Diaphysis, 1/3, distal	48.5	0-48.5
Descending the stairs	Diaphysis, 1/3, distal	31.3	0-31.3
Stand up	Comp. screw entry region	27.1	0-27.01
Sitting	Comp. screw entry region	26.9	0-26.9
Standing on one leg	Femoral head cortex tissue	28.9	0-28.9
Kneeling	Comp. screw entry region	26.7	0-26.7

in the activities, it is seen that the highest stress occurs during the stair climbing, according to the analysis results, although the highest force occurs during stair climbing (2000 N; 370 N, 292 N, 1944 N). Although the total resultant force is 1900 N at the time of climbing the stairs, if it is

Table 8
Femur cortex tissue strain caused by activities

Cortex tissue		
Activity	**Max. strain zone**	**Max. strain**
Walking	Femoral Head Cortex Tissue	0,003
Climbing the stairs	Diaphysis, 1/3, Distal	0,043
Descending the stairs	Femoral Head Cortex Tissue	0,0036
Stand up	Comp. Screw Entry Region	0,0029
Sitting	Comp. Screw Entry Region	0,0029
Standing on one leg	Femoral Head Cortex Tissue	0,0036
Kneeling	Comp. Screw Entry Region	0,0029

Table 9
Spongios cortex tissue stress caused by activities

Cortex tissue			
Activity	**Max. stress zone**	**Max. stress**	**Stress distribution**
Walking (4 km/h)	Spongios tissue groove region	36.5	0-36.5
Climbing the stairs	Spongios tissue groove region	38.55	0-38.55
Descending the stairs	Spongios tissue groove region	38.3	0-38.3
Stand up	Spongios tissue groove region	38.5	0-38.5
Sitting	Spongios tissue groove region	38.2	0-38.2
Standing on one leg	Spongios tissue groove region	38.55	0-38.55
Kneeling	Spongios tissue groove region	37.9	0-37.9

Table 10
Spongios cortex tissue strain caused by activities

Cortex tissue		
Activity	**Max. strain zone**	**Max. strain**
Walking	Spongios tissue groove region	0.051
Climbing the stairs	Spongios tissue groove region	0.052
Descending the stairs	Spongios tissue groove region	0.052
Stand up	Spongios tissue groove region	0.052
Sitting	Spongios tissue groove region	0.052
Standing on one leg	Spongios tissue groove region	0.051
Kneeling	Spongios tissue groove region	0.051

assumed the z-axis vertically, it is 48.5 MPa in the distal part of 1/3 of the diaphysis due to the 464 N in the z direction (towards the posterior direction with respect to the human body) per femur, as seen in Table 8. Equivalent von Misses stress.

Although this value is higher than the 31.3 MPa stress caused by the force (the highest resultant force) at the moment of descending the stairs, it is approximately 1/3 of the stress value of 135 MPa [8], which is the ultimate tensile strength of the bone. The maximum stress on the spongiosteal tissue due to the forces formed according to the activities is 38 MPa on average, which is considered appropriate according to the compact structure of the bone and ultimate tensile strength in the literature. The cortex tissue numerical model of the femur bone is made with orthotropic material modeling. In order to understand the importance of realistic and accurate numerical modeling; the femoral cortex tissue is also modeled as an isotropic material model.

In this cortex tissue material isotropic modeling; the loads that create the maximum tension (48.5 MPa) in the cortex tissue at the time of climbing stairs are modeled as orthotropic and the stress result was evaluated. The stress results of the isotropic femur cortex material numerical model using ANSYS is shown in Fig. 17, a. While the maximum stress created by the forces occurring in the femoral cortex tissue during stair climbing is 48.5 MPa in orthotropic (femur cortex) modeling, it is 92.6 MPa under the same loads n isotropic (femur cortex) modeling. This situation shows that it is a matter to be considered when performing numerical modeling of bone material. The total deformation in the implanted system is investigated. It is observed that there is maximum total deformation of the femoral head for each activity. The highest, maximum deformation (18 mm) occurs when climbing stairs. The result of the total deformation caused by the forces occurring at the moment of climbing the stairs is given in Fig. 17, b.

The maximum deformation caused by the forces on the femoral head as a result of walking, climbing stairs, descending stairs, standing up, sitting, standing on one leg, kneeling is given in Table 11. The mechanical behavior of the nail is important in the static analysis of the implant system. In a structure consisting of nails and long bones, if the rigidity of the implanted nail is too high compared to the bone, a large part of the force coming to the bone implant

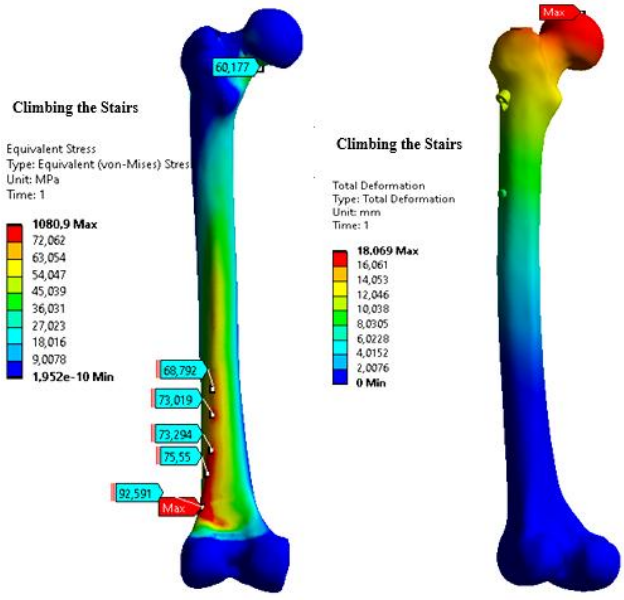

a b

Fig. 17 Stress and deformation results of climbing stairs: a – the result of the stress, b – the result of the total deformation

Table 11

Maximum total deformation amounts occurring in the femoral head according to the activities

Activity	Total deformation, mm
Walking	10.7
Climbing the stairs	18
Descending the stairs	12
Stand up	6
Sitting	2.5
Standing on one leg	7
Kneeling	3.2

system can be carried by the nail and as a result, the bone healing time can be prolonged. In addition, the bone may be in danger of breaking again. In order for the bone healing period to occur in a healthy and effective manner, the incoming loads must be shared at the optimum level in the structure consisting of the implant and bone, and the bone must be exposed to some micro-mobility.

In order for the fracture healing period to occur in a positive and effective manner, the incoming forces must be optimally distributed in the system consisting of the implant and bone, and the bone structure must be exposed to some micro-mobility. The stress state created by the forces occurring in the nail system during the actions of walking, climbing the stairs, and descending the stairs is as in Fig. 18; the stress distribution due to the forces occurring in standing up, sitting, standing on one leg, and kneeling is as in Fig. 19. In the stress distributions seen in Figs. 18-19, stress measurements are taken from 5 critical points for each activity. According to this result, maximum stresses between 110.3 MPa and 165.8 MPa occur in the compression screw pair holes determined on the nail, depending on the activity. Since the yield stress of the implant material using Ti6Al4V Grade 23 ELI titanium alloy is 920 MPa, the nail design has a factor of safety of 5.5 at the most critical point.

In addition, the highest stress state in the 4-degree bending region in the nail design suitable for bone anatomy is 62.2 MPa and is in the act of climbing stairs. In general, in an optimum design, it is desired to distribute the load values homogeneously over the geometry. In Fig. 19, the mentioned homogeneity is seen when the stress distribution that

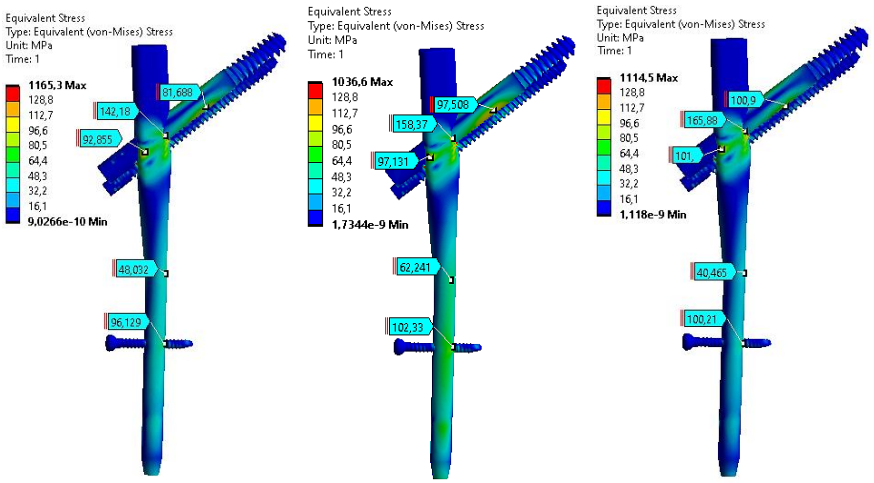

a b c

Fig. 18 The stress state created by the forces occurring in the nail system during the actions: a – walking, b – climbing the stairs, c – descending the stairs

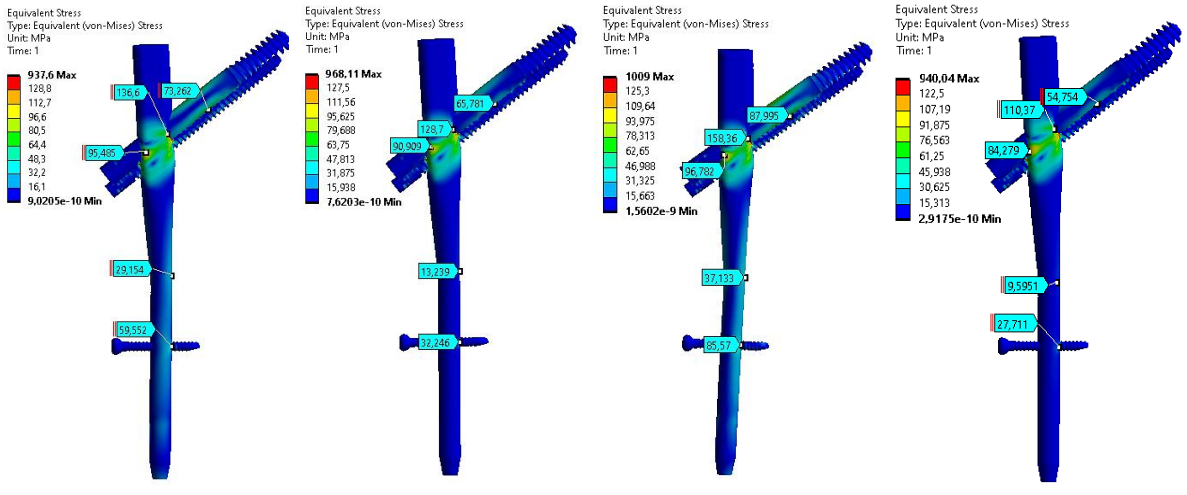

a b c d

Fig. 19 The stress distribution due to the forces occurring the actions: a – stand up, b – sitting, c – standing on one leg, d – kneeling

occurs during the most critical action, which is the climbing stair, is roughly examined. The bending mechanics of the nail is very important in intramedullary nail systems due to the micro deformations that the femur bone is exposed to due to its geometry. As a result of the research, it has been reached that the ASTM F1264 test standard offers an approach in terms of bending for intramedullary nail systems. It is seen that the standard content includes support ranges, loading conditions and bending at 4 points. In this study, the nail system designed is subjected to bending at 3 points due to its geometry. The mesh model of the 3-point bending analysis is given in Fig. 20.

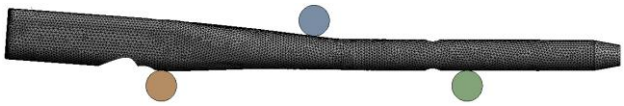

Fig. 20. 3-point bending mesh model

The support spacing is 50 mm and the load is given as 10 mm displacement from the upper support. The two supports at the bottom are fixed. Support conditions are given in Fig. 21, a. Bearings are defined as inter-nail friction and a metal/metal friction coefficient of 0.3 is given. The force corresponding to the yield point is 6690 N in the Y direction and as in Fig. 21, b.

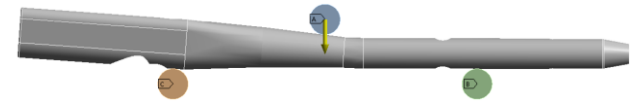

a

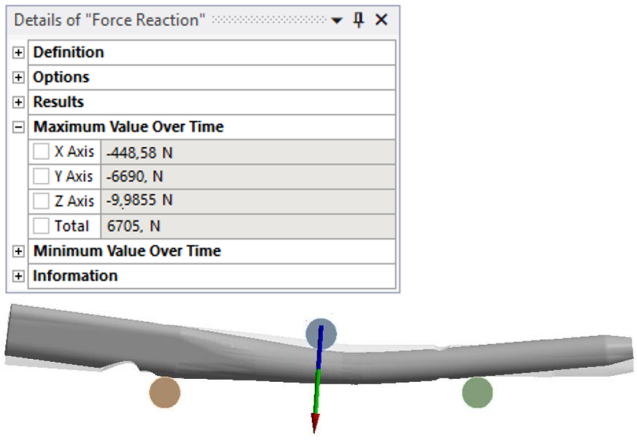

b

Fig. 21 Bending model: a – three support conditions, b – force corresponding to the yield point

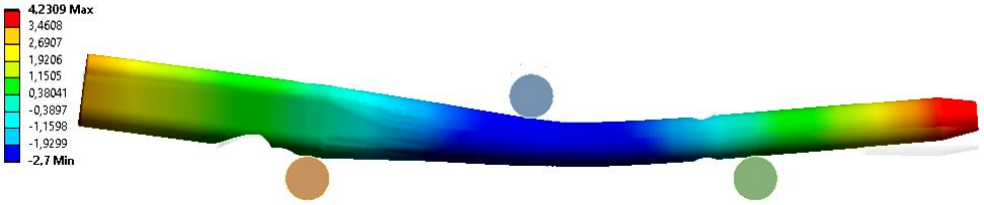

Fig. 22. Displacement in the Y direction corresponding to the yield point

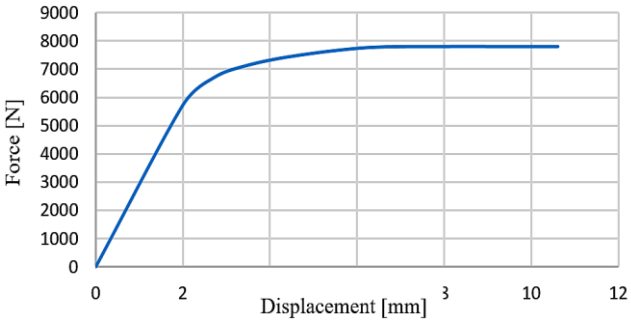

Fig. 23. 3-point bending force-displacement graph

The displacement in the Y direction corresponding to the yield point is 2.7 mm in the load region of the nail, as in Fig. 22.

Fig. 23 shows force-displacement graph. The bending stiffness K, is calculated from the force-displacement plot and is found as 2477.77 N/mm.

The elastic strain corresponding to the yield point in the 3-point bending analysis is given in Fig. 24. In the 3-point bending analysis, the elastic strain values at the yield point are examined and found appropriate.

Plastic strain distribution at yield point in 3-point bending analysis; it is important because it is the point that determines the bending stiffness. In the 3-point bending analysis, the plastic strain distribution corresponding to the yield point is as in Fig. 25. The maximum bending moment is shown in Fig. 26. This is where the importance of modeling

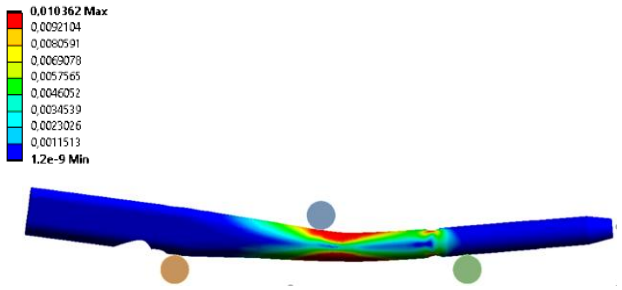

Fig. 24. Elastic strain at yield point

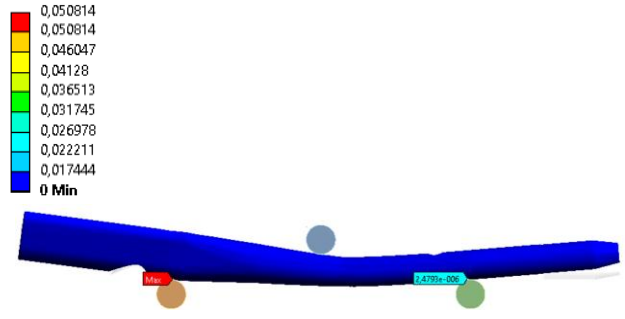

Fig. 25. Plastic strain at yield point

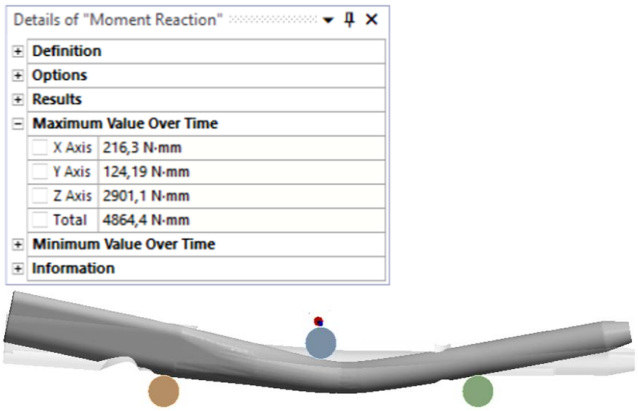

Fig. 26 The maximum bending moment

the material's multi-linear plastic region emerges. When the plastic strain at the yield point is examined, the nail is not subjected to plastic deformation at the yield point. Only small plastic deformation zones are visible at the support contact points. The bending moment at the yield point is 2901.01 N.mm in the Z direction. This moment is also the maximum bending moment. According to the scenario of the 3-point bending test, it is obvious that after the displacement reaches its maximum as the load progresses, it will remain at the maximum for a short time and then the two fixed supports will not be able to create a reaction due to bending and will be reset.

4. Conclusions

Femoral neck fracture cases are seen almost all over the world. There are several different treatment methods for these cases, especially in elderly people. Intramedullary nailing is an advantageous method compared to other methods accepted by the whole world. The most important features for intramedullary nails are; are the materials and designs from which they are produced. Intramedullary nails are generally produced from titanium and its alloys and/or stainless steel materials according to their usage areas. In a suitable nail design, the intramedullary nail must conform to the bone geometry and fit properly into the bone marrow where it is placed. However, although titanium and its alloys provide sufficient stability for the fixation of the fractures, they may behave more rigidly than necessary due to differences in implant designs and material properties, which can create an undesirable result in most fracture treatments and adversely affect the treatment process. First of all, it is important to make an appropriate design so that these results do not occur and then surgery operators and orthopedic doctors do not have difficulty in implanting nail, screw, plate systems during surgery. With the designed implants, it is aimed that the load distribution of the bone implant system is homogeneous. How the implant system behaves under different actions (loads) to model bone tissues as close to reality as possible has been studied.

In this study, it is aimed to provide the fixation of the two broken parts with the compression feature of the designed screw couple placed on the femoral neck, to eliminate the rotational movement in the femoral neck axis and to provide high stability in the single screw systems implanted in the femoral neck. The implant system designed in the study and the implanted state of the bone structure, the stress and strains created by the forces occurring in the femoral head as a result of daily routine movements such as walking, climbing stairs, descending stairs, standing up, sitting, standing on one leg, kneeling, and the 3-point bending test structural analysis results are presented.

In the results of the proposed study;

• It is concluded that true and accurate numerical material modeling of bone tissues should be made.

• Fracture of the femoral neck is modeled and it is observed that the stresses that the femoral bone-implanted system is exposed to as a result of daily actions are homogeneously distributed.

• The importance of multilinear isotropic modeling of Ti6Al4V Grade 23 ELI material has been reached in order to correctly interpret the structural analysis results and see possible risks in the implanted system.

• The result of the 3 point bending structural analysis is interpreted to determine the proper flexibility of the proximal femoral nail together with the bone. Although a local peak stress value of approximately 1114 MPa appeared in the finite element analysis, this was identified as a numerical artifact resulting from mesh discontinuity and contact singularity near the screw–bone interface. When averaged over the surrounding elements, the actual maximum stress in the cortical bone remained below 50 MPa, which is well within physiological limits.

As a result, within the scope of this work, very important technical findings are obtained for the advantageous design of the proximal femoral nail and screws used in the treatment of femoral neck fractures and the biomechanical compatibility of the structure formed by the PFN system with the bone. Although the proximal femoral nail and screw designs in the study are aimed at femoral neck fracture treatments; with the adaptive design change, nail design can be made that can be used in cases of multiple fractures in both the femoral shaft and the femoral diaphysis (shaft). In addition, the material modeling methods and design techniques used in the study will contribute to the literature for similar implant and hip prosthesis designs. It should not be forgotten that the bone structure of human beings changes depending on race, age, gender, weight, level of sports activity, nutritional conditions and living conditions.

Acknowledgement

We would like to thank the Özova Medical Devices Company for their contribution to the study.

References

1. **Bayraktar, H. H.; Morgan, E. F.; Niebur, G. L.; Morris, G. E.; Wong, E. K.; Keaveny, T. M**. 2004. Comparison of the elastic and yield properties of human femoral trabecular and cortical bone tissue, Journal of Biomechanics 37(1): 27-35. https://doi.org/10.1016/S0021-9290(03)00257-4.
2. **Steinberg, E. L.; Blumberg, N.; Dekel, S.** 2005. The fixion proximal femur nailing system: biomechanical properties of the nail and a cadaveric study, Journal of Biomechanics 38(1): 63-68. https://doi.org/10.1016/j.jbiomech.2004.03.014.
3. **Helwig, P.; Faust, G.; Hindenlang, U.; Kroplin, B.; Eingartner, C.** 2006.Finite element analysis of a bone-implant system with the proximal femur nail,

Technology and Health Care 14(4-5): 411-419. https://doi.org/10.3233/THC-2006-144-522.
4. **Tupis, T. M.; Altman, G. T.; Altman, D. T.; Cook, H. A.; Miller, M. C.** 2012. Femoral bone strains during antegrade nailing: A comparison of two entry points with identical nails using finite element analysis, Clinical Biomechanics 27(4): 354-359. https://doi.org/10.1016/j.clinbiomech.2011.11.002.
5. **Freitas, A.; Costa, H. I.; Silva, C. J.; Rangel, C. H. C.** 2013. Static load test of the modified sliding hip screw: The DHS-AF, Acta Ortopédica Brasileira 21(5): 251-254. https://doi.org/10.1590/S1413-78522013000500001.
6. **Bayoglu, R.; Okyar, A. F.** 2015. Implementation of boundary conditions in modeling the femur is critical for the evaluation of distal intramedullary nailing, Medical Engineering and Physics 37(11): 1053-1060. https://doi.org/10.1016/j.medengphy.2015.08.007.
7. **Filardi, V.** 2017. Characterization of an innovative intramedullary nail for diaphyseal fractures of long bones. Medical Engineering and Physics 49: 94-102. https://doi.org/10.1016/j.medengphy.2017.08.002.
8. **Gok, K.; Inal, S.; Gok, A.; Gulbandilar, E.** 2017. Comparison of effects of different screw materials in the triangle fixation of femoral neck fractures, Journal of Materials Science: Materials in Medicine 28: 81. https://doi.org/10.1007/s10856-017-5890-y.
9. **Kwak, D. K.; Kim, W. H.; Lee, S. J.; Rhyu, S. H.; Jang, C. Y.; Yoo, J. H.** 2018. Biomechanical Comparison of Three Different Intramedullary Nails for Fixation of Unstable Basicervical Intertrochanteric Fractures of the Proximal Femur: Experimental Studies, BioMed Research International 2018: 7618079. https://doi.org/10.1155/2018/7618079.
10. **Putame, G.; Pascoletti, G.; Terzini, M.; Zanetti, E. M.; Audenino, A. L.** 2020. Mechanical Behavior of Elastic Self-Locking Nails for Intramedullary Fracture Fixation: A Numerical Analysis of Innovative Nail Designs, Frontiers in Bioengineering and Biotechnology 8: 557. https://doi.org/10.3389/fbioe.2020.00557.
11. **Herrera, A.; Rosell, J.; Ibarz, E.; Albareda, J.; Gabarre, S.; Mateo, J.; Gracia, L.** 2020. Biomechanical analysis of the stability of anterograde reamed intramedullary nails in femoral spiral fractures, Injury 51: S74-S79. https://doi.org/10.1016/j.injury.2020.02.034.
12. **Wang, J.; Ma, J. X.; Lu, B.; Bai, H. H.; Wang, Y.; Ma, X. L.** 2020. Comparative finite element analysis of three implants fixing stable and unstable subtrochanteric femoral fractures: Proximal Femoral Nail Antirotation (PFNA), Proximal Femoral Locking Plate (PFLP), and Reverse Less Invasive Stabilization System (LISS), Orthopaedics & Traumatology: Surgery & Research 106(1): 95-101. https://doi.org/10.1016/j.otsr.2019.04.027.
13. **Solórzano, W.; Ojeda, C.; Diaz Lantada A.** 2020. Biomechanical Study of Proximal Femur for Designing Stems for Total Hip Replacement, Applied Sciences 10(12): 4028. https://doi.org/10.3390/app10124028.
14. **Bergmann, G.; Graichen, F.; Rohlmann, A.; Bender, A.; Heinlein, B.; Duda, G. N.; Heller, M. O.; Morlock, M. M.** 2010. Realistic loads for testing hip implants, Bio-Medical Materials and Engineering 20(2): 65-75. https://doi.org/10.3233/BME-2010-0616.

H. H. Gökmen, M. Tınkır, A. Öztürk

STRUCTURAL ANALYSIS OF NOVEL DESIGN COMPRESSION FEATURE INTRAMEDULLARY NAIL SYSTEM USED IN TREATMENT OF FEMORAL NECK BONE FRACTURE

S u m m a r y

In this study, the design, numerical modeling, and static analysis of an intramedullary nail system with a compression feature developed to treat femoral neck fractures and prevent rotational displacement of the fractured parts were performed. Three-dimensional models were created considering the mechanical properties of cortical (stiff) and spongious (soft) bone tissues, and a fracture profile was designed in the femoral head. The nail system, manufactured from Ti6Al4V Grade 23 alloy, was implanted virtually into the femur to achieve stable fixation.

Two material models, isotropic and orthotropic, were used for representing the femur bone, and it was concluded that the orthotropic model provided results more consistent with the literature. Structural analyses of both the intramedullary nail system and femur bone were carried out using the finite element method (FEM) under various loading scenarios representing daily human activities such as walking, stair climbing/descending, standing, sitting, kneeling, and one-leg stance. Additionally, a three-point bending test according to ASTM F1264 standards was simulated to evaluate the rigidity of the nail.

The maximum stress on the nail was obtained as 158.37 MPa during stair climbing and 165.88 MPa during stair descending, while the maximum deformation of 18 mm occurred in the nail system under compression. The results demonstrate that the proposed design ensures high mechanical stability and effective load transfer, providing a promising alternative for femoral neck fracture treatment.

Keywords: femoral neck fracture, intramedullary nail system, compression, isotropic and orthotropic bone material model, deformation, stress-strain, finite element analysis.

Received December 11, 2022
Accepted December 15, 2025